

CALIBRATION OF HIGHER FREQUENCY CHARACTERISTICS OF GEOPHONE

By

Chōrō KITSUNEZAKI

(Received November 30, 1967)

Abstract

In this paper the author developed the new method to calibrate the geophone characteristics in the higher frequency range, where exact measurement can not be assured by all most all methods developed in usual lower frequency range.

When the longitudinal wave propagates along one dimensional bar, we can evaluate its particle velocity by detecting its strain. Using this principle, we detect the vibration velocity of the geophone body (to be tested) attached to the end of the bar.

The merit of this method is that we can check the setting condition of the geophone by evaluating the reflection coefficient of the wave at the geophone end.

By this method the author could calibrate the frequency characteristics of geophones up to 3000 or 4000 cps.

Introduction

In usual seismic prospecting, the frequency range of observed seismic waves is relatively low, nearly 5 to 100 cps. Usual wellknown calibration methods can be applied in this frequency range.

However in "high frequency seismic prospecting" which has been studied by the author, the higher frequency range, 100 to 5000 cps, is observed (Kitsunezaki *et al.* [1960], Kitsunezaki [1960a], [1960b], [1961], [1963]).

In such a higher frequency range exact results are not assured by almost all wellknown calibration methods.

This has been one of the fundamental difficulties of the "high frequency seismic prospecting", because exact quantitative discussion on wave properties is difficult without completely calibrated geophones.

There are many reasons to make us expect that real geophone characteristics of higher frequency range shows considerable departure from ideal wellknown characteristics, which is valid in the lower frequency range.

In this paper, a new method to calibrate the geophone in the higher frequency range will be developed.

1. Theory

(1) Principle of the method

Displacement of nondispersive elastic waves which propagate along on one dimensional bar (completely elastic medium) is expressed by the following equation :

$$u = u(t \mp x/C) \quad (1)$$

where u is displacement, t is time, x is distance along the bar, C is propagation velocity. Selection of the symbol “ \mp ” depends on the propagation direction. The upper symbol “ $-$ ” should be used when the waves propagate in the positive direction, the lower symbol in the negative direction.

If we take partial derivatives of u , the following simple relation can easily be found :

$$\frac{\partial u}{\partial t} = \mp C \frac{\partial u}{\partial x}.$$

Particle velocity, $\partial u / \partial t$, shall be expressed as V . strain $\partial u / \partial x$ as ϵ :

$$V = \mp C \epsilon. \quad (2)$$

From this relation, the particle velocity can easily be evaluated by measuring the strain. Generally, direct measuring of the particle velocity is difficult in the higher frequency range. The strain, however, can be easily measured by the strain gauge.

Let us assume that a geophone to be tested is fixed at one end of a long elastic bar (wave bar). The longitudinal elastic wave of short duration is generated at the other end of the bar, for example, simply by striking one end with a small rigid ball. The wave is reflected after incidence to the geophone end. Strain of those incident (ϵ_i) and reflected (ϵ_r) waves is detected by a set of strain gauges which is adhered to the proper position (S) of the bar (Fig. 1).

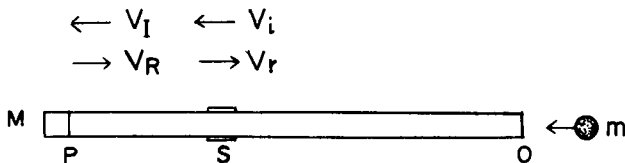


Fig. 1. Illustration of the principle.

From the strains, ϵ_i and ϵ_r , the particle velocities of respective waves can be evaluated, i.e.,

$$V_i = -C \epsilon_i \quad V_r = C \epsilon_r. \quad (3)$$

Positive direction of x is assumed to be incidence direction.

The particle velocities of incident and reflected waves at the reflecting end (i.e., the geophone to be tested) shall be denoted respectively as V_I and V_R .

$$\left. \begin{aligned} V_I &= V_i(t-r/C) \\ V_R &= V_R(t+r/C) \end{aligned} \right\} \quad (4)$$

Let the particle velocity of the geophone body be V , i.e.,

$$V = V_I + V_R. \quad (5)$$

If the response, E (output voltage), of the geophone is detected in this process, the characteristics of the geophone can be evaluated by comparison between E and V .

Symbols with a bar above time function symbols shall be defined as the frequency spectra of original respective time function.

For example,

$$\left. \begin{aligned} \bar{E} &= \bar{E}(\omega) = \int_{t_1}^{t_2} E(t) e^{-j\omega t} dt \\ \bar{V} &= \bar{V}(\omega) = \int_{t_1}^{t_2} V(t) e^{-j\omega t} dt. \end{aligned} \right\} \quad (6)$$

In respective time functions, it is assumed that their values (amplitude) vanish at time range of $t < t_1$ and $t > t_2$. t_1 and t_2 are independently defined in respective functions. ω is angular frequency, i.e., $\omega = 2\pi f$ where f is frequency. $j = \sqrt{-1}$. Frequency characteristics, $\bar{A}(\omega)$, of the tested geophone is defined as follows:

$$\bar{A}(\omega) = \bar{E}(\omega) / \bar{V}(\omega). \quad (7)$$

This is the fundamental principle of the geophone calibration method, which will be developed in this paper.

(2) Considerations on practical problems

2-1 Attenuation

When this method is applied practically, some modifications become necessary to be introduced.

Though Eq. (1) is valid in completely elastic medium, real bars are not so. Propagating along a bar, elastic waves attenuate. In this case, amplitude of a single sinusoidal elastic wave is expressed as follows:

$$u = u_0 e^{\mp \alpha x} e^{j\omega(t \mp x/C)}. \quad (8)$$

As for this equation, u is optional quantity of elastic wave, for example, displacement, particle velocity, strain, etc. u_0 is constant. α is attenuation constant which generally depends of frequencies.

Considering the above relation, we can modify Eq. (2) as

$$\frac{\partial u}{\partial t} = \mp \frac{C}{1 \mp j \frac{\delta}{2\pi}}$$

where

$$\delta \text{ (logarithmic decrement)} = \alpha C / f$$

$$\frac{\partial u}{\partial t} = \mp \frac{C}{\sqrt{1 + (\delta/2\pi)^2}} \frac{\partial u}{\partial x} e^{\mp j\delta/(2\pi)}. \quad (9)$$

Generally, $\delta/(2\pi)$ is sufficiently less than 1. Therefore, Eq. (2) is practically valid.

In stead of Eq. (4), the following equations are given by Eq. (8) :

$$\left. \begin{aligned} V_I &= e^{-\alpha r} e^{-j\omega r/C} \bar{V}_i(\omega) \\ V_R &= e^{\alpha r} e^{j\omega r/C} \bar{V}_r(\omega), \end{aligned} \right\} \quad (10)$$

where

$$\begin{aligned} \bar{V}_i(\omega) &= \int_{t_1}^{t_2} V_i(t) e^{-j\omega t} dt \\ \bar{V}_r(\omega) &= \int_{t_1}^{t_2} V_r(t) e^{-j\omega t} dt. \end{aligned}$$

r is the distance between P and S (Fig. 1).

$$\left. \begin{aligned} \bar{V}_I &= |\bar{V}_I| e^{j\theta_I} = Re(\bar{V}_I) + jIm(\bar{V}_I), \\ |\bar{V}_I| &= e^{-\alpha r} |\bar{V}_i| \\ \theta_I &= \theta_i - \omega r / C. \end{aligned} \right\} \quad (11)$$

where

$$\left. \begin{aligned} \bar{V}_R &= |\bar{V}_R| e^{j\theta_R} = Re(\bar{V}_R) + jIm(\bar{V}_R), \\ |\bar{V}_R| &= e^{\alpha r} |\bar{V}_r| \\ \theta_R &= \theta_r + \omega r / C. \end{aligned} \right\} \quad (12)$$

Re and Im mean real and imaginary parts, i.e.,

$$\left. \begin{aligned} Re(\bar{V}_I) &= |\bar{V}_I| \cos \theta_I & Im(\bar{V}_I) &= |\bar{V}_I| \sin \theta_I \\ Re(\bar{V}_R) &= |\bar{V}_R| \cos \theta_R & Im(\bar{V}_R) &= |\bar{V}_R| \sin \theta_R. \end{aligned} \right\} \quad (13)$$

Eq. (5) is also valid in the case of attenuating wave, i.e.,

$$\begin{aligned} \bar{V} &= \bar{V}_I + \bar{V}_R \\ &= \{Re(\bar{V}_I) + Re(\bar{V}_R)\} + j\{Im(\bar{V}_I) + Im(\bar{V}_R)\}. \end{aligned} \quad (14)$$

2-2 Reflection coefficient

It is assumed that the geophone body is regarded as a rigid body (mass: M). Acoustic impedance is generally defined as the ratio of the force acting on the body to its velocity. Acoustic impedance of the geophone body, Z_M , is

given as

$$\bar{Z}_M = j\omega M.$$

Acoustic impedance of the elastic bar, \bar{Z}_R , is given as

$$\bar{Z}_R = \rho CS,$$

where ρ is density of the bar, S is its sectional area.

Reflection coefficient, \bar{r} , of the elastic wave at the end of the bar attached to the rigid body is expressed by the following equation :

$$\bar{r} = \frac{-\bar{V}_R}{\bar{V}_I} = \frac{j\omega M - \rho CS}{j\omega M + \rho CS}.$$

$$\frac{\bar{V}_R}{\bar{V}_I} = -\bar{r} \equiv |\bar{r}| e^{j\theta_r},$$

where

$$|\bar{r}| = 1, \quad \theta_r = -2 \tan^{-1} \frac{\omega M}{\rho CS}. \quad (15)$$

θ_r is also expressed by phase angles of \bar{V}_R and \bar{V}_I , else by \bar{V}_r and \bar{V}_i :

$$\begin{aligned} \theta_r &= \theta_R - \theta_I \\ &= \theta_r - \theta_i + 2\omega r / C. \end{aligned} \quad (16)$$

$$\begin{aligned} \bar{V} &= \bar{V}_I + \bar{V}_R = \bar{V}_I (1 + \bar{V}_R / \bar{V}_I) \\ &= \bar{V}_I (1 - \bar{r}). \end{aligned} \quad (17)$$

$$\begin{aligned} 1 - \bar{r} &= \frac{2}{1 + \frac{j\omega M}{\rho CS}} \\ &= \frac{2}{\sqrt{1 + \left(\frac{\omega M}{\rho CS}\right)^2}} e^{j\theta_r / 2}. \end{aligned} \quad (18)$$

From Eq. (11) and Eq. (12), the following relation is obtained :

$$|\bar{V}_R| |\bar{V}_I| = |\bar{V}_r| |\bar{V}_i|.$$

Since $|\bar{V}_R| = |\bar{V}_I|$ is obtained by Eq. (15),

$$|\bar{V}_I|^2 = |\bar{V}_r| |\bar{V}_i|.$$

Hence

$$\begin{aligned} \log |\bar{V}_I| &= \frac{1}{2} \{ \log |\bar{V}_i| + \log |\bar{V}_r| \} \\ &= \log C + \frac{1}{2} \{ \log |\bar{\epsilon}_i| + \log |\bar{\epsilon}_r| \}. \end{aligned} \quad (19)$$

$\frac{1}{2} \{ \log |\bar{\epsilon}_i| + \log |\bar{\epsilon}_r| \}$ is mean value of $\log |\bar{\epsilon}_i|$ and $\log |\bar{\epsilon}_r|$. $|\bar{V}_I|$ can be estimated directly from observation values, $\bar{\epsilon}_i$ and $\bar{\epsilon}_r$, without knowledge of attenuation constant α , as far as Eq. (15) is valid.

2-3 Separation of High Frequency Characteristics

Since length of the real bar is finite, incident and reflected waves repeatedly propagate. In order to analyze the geophone characteristics completely, obstruction by repeated reflection should be excluded. If the time (t_H) for the wave to propagate along the whole length of the bar is sufficiently longer than the wave pulse duration and the duration of the geophone response, necessary consideration has been completed by the previous discussion.

The wave pulse duration can be easily made shorter than the above propagation time. It is, however sometimes, difficult to make the bar longer than the length (l_p) which corresponds to the geophone response duration (t_p) (l_p is defined as $l_p=Ct_p$). For example, in the following experiment the propagation velocity (C) of longitudinal wave is 1.64 km/s. Natural frequency of the geophone (moving coil type) is about 30 cps, damping constant is about 0.4. Practical duration of the geophone response is one natural period, about 3.3×10^{-2} s, if sufficiently short wave pulse is impressed. The length corresponding to this duration is $3.3 \times 10^{-2} \text{ s} \times 1.64 \times 10^3 \text{ m/s} = 54 \text{ m}$. The time which corresponds to one round trip of the wave along whole length of the bar is free from the reflection waves coming succeedingly. Hence, necessary length of the bar is $l_p/2$, i.e., 27 m. In usual laboratory condition it is difficult to set such a long

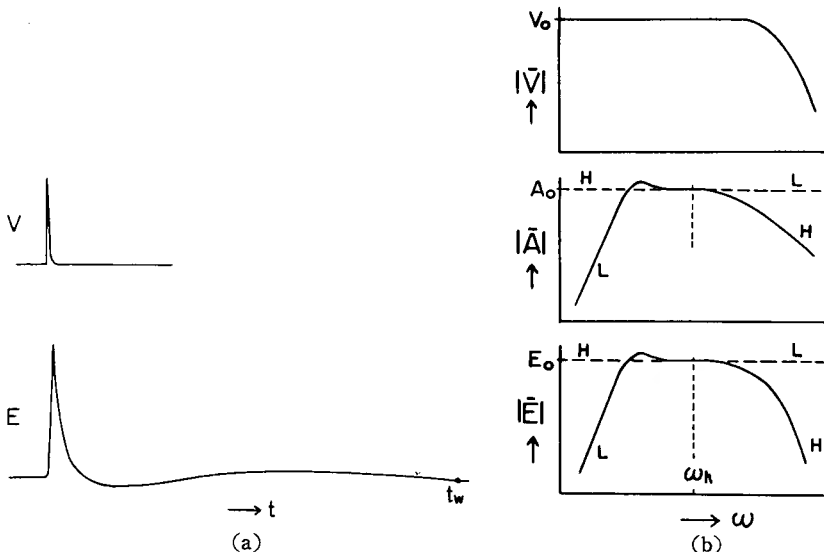


Fig. 2. (a) Input signal (V : particle velocity) and output response (E) of the tested geophone.

(b) Relation of the input and output spectra of the geophone.

\bar{V} : input spectrum

\bar{A} : characteristics of the geophone,

\bar{E} : output spectrum,

$H-H$; $A_0\bar{A}_H$, $L-L$; $A_0\bar{A}_L$.

$H-H$; $E_0\bar{E}_H$, $L-L$; $E_0\bar{E}_L$.

bar.

Further consideration should be paid not only to the response duration of the geophone, but to the attenuation property of the bar. The velocity of the bar (vinyl chloride) cited in the previous example is very low, compared with usual materials. Generally, low velocity materials are also high loss materials. Also from this view point, the length of the bar should be restricted. Therefore, it is not easy to get the complete geophone response in usual condition, owing to the restrictions of the bar length.

For convenience of illustration it shall be assumed that the tested geophone is moving coil type. In Fig. 2, the input signal (particle velocity of the geophone body) and the output response (output voltage of the geophone) are schematically demonstrated as an ideal state. The information of the higher frequency characteristics of the geophone will be concentrated in the earlier short period of the whole response duration. Therefore we can have hope to make the necessary higher frequency information free from the obstruction of succeeding disturbance excited by the reflection waves. The lower frequency characteristics is usual geophone characteristics itself, which can be measured by variable well-known methods.

In the next step, we shall study how to separate the higher and the lower frequency response from the geophone response $E(t)$.

Frequency characteristics of the geophone, $\bar{A}(\omega)$, is conveniently expressed in the following form :

$$\left. \begin{aligned} \bar{A}(\omega) &= A_0 \bar{A}_L(\omega) \bar{A}_H(\omega) \\ \bar{A}(\omega) &= \bar{E}(\omega) / \bar{V}(\omega) \end{aligned} \right\} \quad (20)$$

\bar{A}_L and \bar{A}_H respectively mean so-called "low cut" and "high cut" characteristics. In sufficiently higher frequency range $\bar{A}_L(\omega)=1$, in moderately low frequency range it shows particular form, and in further lower frequency range $\bar{A}_L(\omega)=0$. \bar{A}_H has the reverse characteristics compared with \bar{A}_L . A_0 is absolute magnitude of \bar{A} . $A_0 \bar{A}_L(\omega)$ is the geophone characteristics in general meaning, which is familiar to the seismologist, $\bar{A}_H(\omega)$ can be considered as a correction factor which becomes effective in the higher frequency range. Their meanings are schematically illustrated in Fig. 2.

Input signal $\bar{V}(\omega)$ is also written as

$$\bar{V}(\omega) = V_0 \bar{V}_L(\omega) \bar{V}_H(\omega). \quad (21)$$

The meanings of V_0 , \bar{V}_L and \bar{V}_H correspond to A_0 , \bar{A}_L and \bar{A}_H respectively. In the real experiment a single pulse deflecting in one direction can be obtained. Hence we can make

$$\begin{aligned}\bar{V}_L &= 1 \\ \bar{V} &= V_0 \bar{V}_H(\omega).\end{aligned}\quad (22)$$

Considering the relation :

$$\bar{E} = \bar{A} \bar{V}, \quad (23)$$

we shall define

$$\begin{aligned}E_0 &= A_0 V_0 \\ \bar{E}_H &= \bar{A}_H \bar{V}_H \\ \bar{E}_L &= \bar{A}_L.\end{aligned}\quad (24)$$

Hence

$$\bar{E} = E_0 \bar{E}_H \bar{E}_L. \quad (25)$$

E_0 , \bar{E}_L and \bar{E}_H have the meanings corresponding to A_0 , \bar{A}_L and \bar{A}_H respectively. In Eq. (25) \bar{E} is expressed as the product of \bar{E}_L and \bar{E}_H . Direct application of such a form is not convenient to separate both the characteristics, \bar{E}_L and \bar{E}_H , from the real response, $E(t)$. Eq. (25) shall be modified in the form of the sum of two informations in the succeeding step.

$$\begin{aligned}\bar{E} &= E_0 \bar{E}_L \bar{E}_H \\ &= E_0 \{ \bar{E}_L - \bar{E}_L (1 - \bar{E}_H) \} \\ &= E_0 \{ 1 - \bar{E}_L (1 - \bar{E}_H) - (1 - \bar{E}_L) \} \\ &= E_0 \{ \bar{E}_H - \bar{E}_L \},\end{aligned}\quad (26)$$

where

$$\left. \begin{aligned}\bar{E}_H &= 1 - \bar{E}_L (1 - \bar{E}_H) \\ \bar{E}_L &= 1 - \bar{E}_L\end{aligned} \right\} \quad (27)$$

or

$$\left. \begin{aligned}\bar{E}_H &= 1 + \frac{\bar{E}_H - 1}{\bar{E}_L} \\ \bar{E}_L &= 1 - \bar{E}_L.\end{aligned} \right\} \quad (28)$$

Inverse Fourier transformation of Eq. (26) is

$$E(t) = E_0 \{ E_h(t) - E_l(t) \}, \quad (29)$$

where

$$E(t) = \int_{-\infty}^{+\infty} \bar{E}(\omega) e^{j\omega t} d\omega.$$

Other quantities are also defined in the same fashion. From Eq. (29)

$$E_0 E_h(t) = E(t) + E_0 E_l(t). \quad (30)$$

It is expected that $E_l(t)$ will be evaluated from the lower frequency characteristics, $\bar{E}_L(\omega)$.

It shall be assumed that \bar{E}_L follows the usual differential equation of the

second order, so-called vibration equation. This assumption may be very natural. Wellknown equation regarding the motion of moving coil type geophone is expressed as follows :

$$\left. \begin{aligned} \frac{d^2y}{dt^2} + 2nh \frac{dy}{dt} + n^2y &= - \frac{d^2x}{dt^2} \\ E &= \frac{GR}{R+R_0} \frac{dy}{dt}, \end{aligned} \right\} \quad (31)$$

where R_0 is internal (coil) resistance, R is load resistance, G is force factor (voltage sensitivity), h is damping constant, n is natural angular frequency, y is displacement of the coil (pendulum) relative to the geophone body, x is displacement of the geophone body, E is output voltage. In damping constant, h , of Eq. (31), electromagnetic effect caused by coil current is also included, i.e.,

$$h = h_0 + h_e, \quad h_e = G^2 / \{2mm(R + R_0)\},$$

where h_0 is damping constant at open circuit, h_e is damping constant caused by coil current, m is mass of the pendulum.

If the input

$$\frac{dx}{dt} = V = V_0 e^{j\omega t} \quad (32)$$

is impressed on the system expressed by Eq. (31), we have the output response as follows.

$$E = -V_0 \frac{GR}{R+R_0} \frac{e^{j\omega t}}{1 - \left(\frac{n}{\omega}\right)^2 - j2h\left(\frac{n}{\omega}\right)}. \quad (33)$$

From Eq. (32) and (33), it is easily found that the output response to the input, $\bar{V} = V_0$, is

$$\bar{E} = -V_0 \frac{GR}{R+R_0} \frac{1}{1 - \left(\frac{n}{\omega}\right)^2 - j2h\left(\frac{n}{\omega}\right)}.$$

In such an ideal case, \bar{A} is $A_0 \bar{A}_L$. Hence,

$$\begin{aligned} A_0 &= - \frac{GR}{R+R_0} \\ \bar{A}_L &= \left\{ 1 - \left(\frac{n}{\omega}\right)^2 - j2h\left(\frac{n}{\omega}\right) \right\}^{-1}. \end{aligned} \quad (34)$$

A_L can be directly evaluated from Eq. (34) by "inverse Fourier transformation". In the succeeding step, however, we evaluate A_L by somewhat classic method.

In the preceding discussion, if we put

$$A_0 = 1 \quad \text{and} \quad \frac{dx}{dt} = V = e^{j\omega t} d\omega,$$

E becomes

$$E = A_L e^{j\omega t} d\omega.$$

Hence, when

$$\frac{dx}{dt} = \int_{-\infty}^{\infty} e^{j\omega t} d\omega = \delta(t) \quad (35)$$

is impressed on the system, the output becomes

$$E = \int_{-\infty}^{\infty} A_L e^{j\omega t} d\omega = A_L. \quad (36)$$

In other words, if we impress the input, $dx/dt = \delta(t)$ on the system expressed in the following equation :

$$\frac{d^2 y}{dt^2} + 2nh \frac{dy}{dt} + n^2 y = \frac{d^2 x}{dt^2}, \quad (37)$$

we can obtain A_L as its output, dy/dt .

A_1 shall be defined as the response, dy/dt , of the above system, on which the following input, $d^2 x/dt^2$, is impressed :

$$\frac{d^2 x}{dt^2} = U(t),$$

where

$$U(t) = \begin{cases} 0 & t < 0 \\ 1 & t \geq 0. \end{cases}$$

$A_1(t)$ can be obtained by the classic analysis :

$$A_1 = \begin{cases} U(t) \cdot \frac{e^{-\varepsilon t} \sin \omega_i t}{\omega_i} & : h < 1 \\ U(t) \cdot \frac{e^{-\varepsilon t} \sinh \omega_i t}{\omega_i} & : h > 1 \\ U(t) t e^{-nt} & : h = 1, \end{cases} \quad (38)$$

where

$$\varepsilon = nh, \quad \omega_i = n\sqrt{1-h^2}. \quad (39)$$

If

$$\begin{aligned} \frac{dx}{dt} &= \delta(t) \quad \left(= \frac{dU(t)}{dt} \right), \\ \frac{d^2 x}{dt^2} &= \frac{d^2 U(t)}{dt^2}. \end{aligned}$$

The response of the system expressed in Eq. (37), on which the above input is impressed, is given as :

$$\frac{dy}{dt} = A_L = \frac{d^2 A_1}{dt^2}. \quad (40)$$

As an example, A_L in the case of $h < 1$ shall be evaluated.

$$\begin{aligned} \frac{dA_1}{dt} &= e^{-\epsilon t} \left(\cos \omega t - \frac{h}{\sqrt{1-h^2}} \sin \omega t \right) U(t). \\ \therefore \int_{-0}^t A_L(t) dt &= e^{-\epsilon t} \left(\cos \omega t - \frac{h}{\sqrt{1-h^2}} \sin \omega t \right) U(t). \end{aligned} \quad (41)$$

Based on the same idea as Eq. (26), \bar{A}_L shall be newly defined as

$$\bar{A}_L = 1 - \bar{A}_L$$

From Eq. (24),

$$\bar{A}_L = \bar{E}_L.$$

Inverse Fourier transformation of the above equation gives

$$A_L(t) = \delta(t) - A_L(t). \quad (42)$$

Hence

$$\int_{-0}^t A_L(t) dt = 1 - e^{-\epsilon t} \left(\cos \omega t - \frac{h}{\sqrt{1-h^2}} \sin \omega t \right) U(t). \quad (43)$$

Since

$$\begin{aligned} A_L &= \frac{d^2 A_1}{dt^2} = \delta(t) - 2nh \cdot e^{-\epsilon t} \left(\cos \omega t + \frac{1-2h^2}{2h\sqrt{1-h^2}} \sin \omega t \right) U(t), \\ A_L &= 2\epsilon e^{-\epsilon t} \left(\cos \omega t + \frac{1-2h^2}{2h\sqrt{1-h^2}} \sin \omega t \right) U(t). \end{aligned} \quad (44)$$

By the above equation (44), A_L can be evaluated, if the geophone constants, n and h are given.

Though E_0 can be given by $A_0 V_0 = E_0$, it can be also evaluated by the relations developed in the following discussion.

Effective duration of $E_h(t)$ is generally shorter than whole duration (t_w) of $E(t)$. So we can optionally give the time, t_h , such as,

$$\begin{aligned} t > t_h: & \quad E_h(t) \doteq 0, \\ t_h < t_w. & \end{aligned}$$

Beginning of the input pulse applied to the geophone shall be taken as the origin of time coordinate.

From Eq. (30),

$$\int_{-0}^{\infty} E_0 E_h(t) dt = \int_{-0}^{\infty} E(t) dt + \int_{-0}^{\infty} E_0 E_L(t) dt. \quad (45)$$

From $\bar{E}(0) = A_0 V_0 \bar{A}_L(0) = 0$,

$$\int_{-0}^{\infty} E(t) dt = \bar{E}(0) = 0.$$

Therefore

$$\int_{-0}^{t_h} E_h(t) dt = \int_{-0}^{\infty} E_h(t) dt = \int_{-0}^{\infty} E_l(t) dt. \quad (46)$$

Eq. (43) gives

$$\int_{-0}^{\infty} A_l(t) dt = \int_{-0}^{\infty} E_l(t) dt = 1. \quad (47)$$

From Eq. (46) and Eq. (47),

$$\int_{-0}^{t_h} E_h(t) dt = 1. \quad (48)$$

$$E_0 \int_{-0}^{t_h} E_h(t) dt = \int_{-0}^{t_h} E(t) dt + E_0 \int_{-0}^{t_h} E_l(t) dt.$$

From Eq. (48),

$$E_0 = \int_{-0}^{t_h} E(t) dt + E_0 \int_{-0}^{t_h} E_l(t) dt.$$

Hence

$$E_0 = \frac{\int_{-0}^{t_h} E(t) dt}{1 - \int_{-0}^{t_h} A_l(t) dt} = \frac{\int_{-0}^{t_h} E(t) dt}{\int_{-0}^{\infty} A_l(t) dt}. \quad (49)$$

From the preceding discussion, it is concluded that the higher frequency response $E_h(t)$ can be evaluated by Eq. (30), if the geophone response $E(t)$ is completely obtained in the duration from -0 to t_h . Since $\bar{E}_h(\omega)$ is given by the Fourier transformation from $E_h(t)$, $\bar{E}_H(\omega)$ can be evaluated by Eq. (28).

Generally, we can find ω_h which practically satisfies the following relation :

$$\omega > \omega_h \quad \bar{E}_L = 1. \quad (50)$$

In $\omega > \omega_h$, Eq. (28) becomes simple as follows :

$$\bar{E}_h(\omega) \doteq \bar{E}_H(\omega). \quad (51)$$

2. Experiment

In order to make the author's idea clear, the experiment practically carried out will be demonstrated as an example in this chapter. Experimental procedures are schematically illustrated in Fig. 3.

The wave bar is a cylindrical bar made of vinyl chloride, 1.93 m in length and 3 cm in diameter. A strain detector consists of a pair of strain gauges (2 cm long) adhered to either side of the bar and facing each other. Longitudinal strain along the bar axis was detected with this arrangement. The circuit illustrated in Fig. 3(c) assures detecting only the longitudinal wave free from obstruction of the flexural wave.

The tested geophone (GEOSPACE HSJ-K, natural frequency: 28 cps) was buried in the hole made at the end of the bar and was fixed with the screws

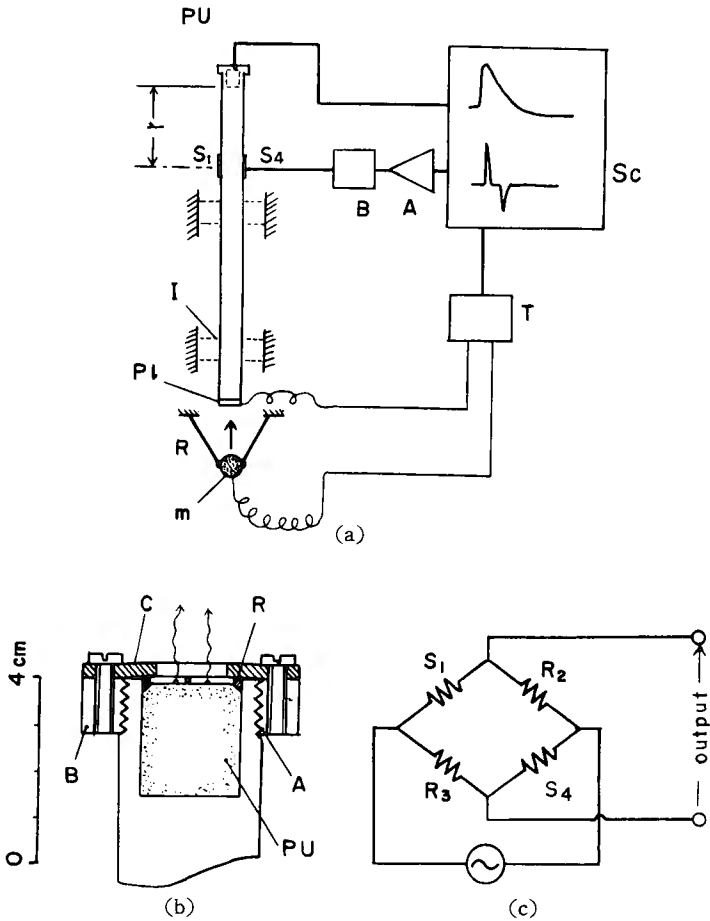


Fig. 3. (a) Illustration of the experimental procedure.

S_1S_4 : strain gauge, B : bridge circuit, A : pre-amplifier,
 Sc : syncroscope, PU : geophone to be tested, I : vibration isolator (sponge),
 R : rubber string, m : rigid (iron) ball, T : trigger circuit,
 Pl : iron plate.

(b) Setting of the geophone to be tested.

PU : geophone body, C : cover plate,
 B : plastic base (adhered at "A"), R : split ring.

(c) Bridge circuit detecting strain.

S_1S_4 : strain gauge, $S_1=S_4=R_2=R_3$.

through the cover plate and the split ring. This feature is also illustrated in Fig. 3.

Longitudinal wave pulse was generated by striking the small iron ball against the end of the wave bar. The iron plate adhered to this end of the bar makes a switch circuit with the iron ball, which closes with their contact and triggers sweep of the syncroscope.

Output signals of the strain detector and the geophone were delivered to the two beam syncroscope and were recorded on a piece of photographic paper with a camera. The wave traces on Fig. 4 are ones plotted from digitalized data. These shall be called the original data. The frequency spectra of the strain traces are shown on Fig. 5. These shall be called the original spectra.

At first we shall investigate the acoustic impedance regarding the real data. The incident strain signal ϵ_i and the reflected strain signal ϵ_r were recorded on

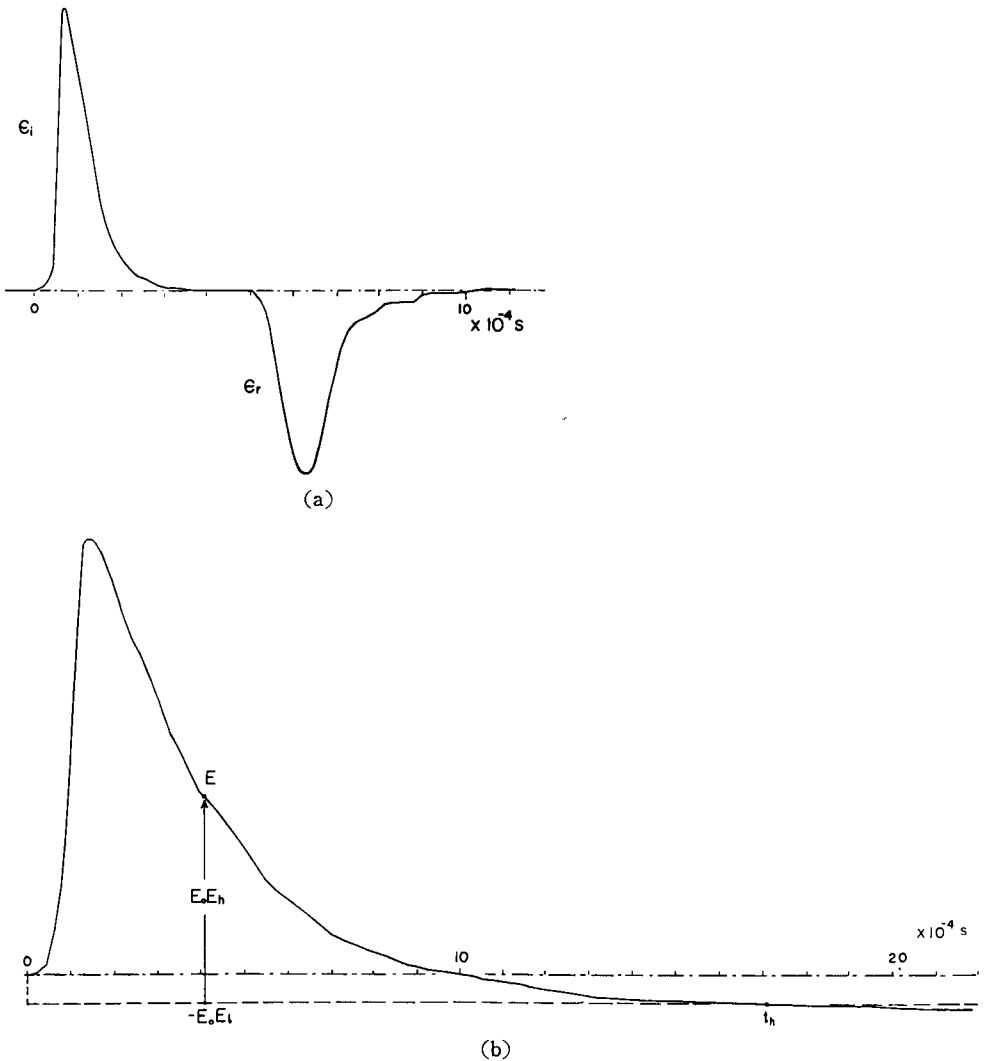


Fig. 4. (a) Record of the incident and reflected strain signal.
 (b) Record of the geophone output obtained as a response to the signals in Fig. 4 (a).
 Setting of the geophone and the wave bar: vertical,
 tested geophone: vertical motion detector (V1).

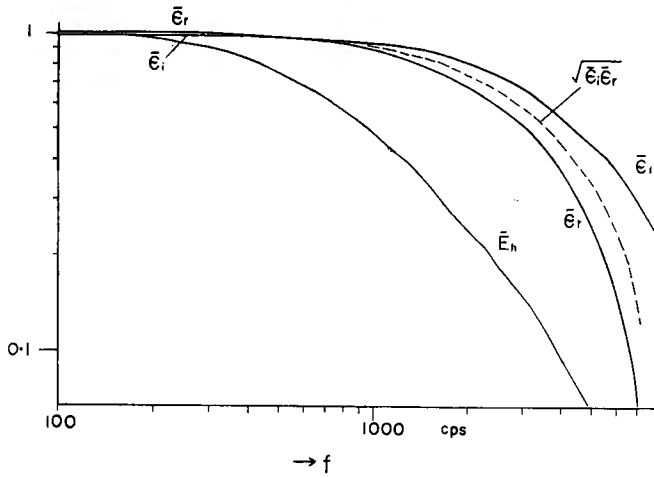


Fig. 5. Spectra of signals. Vertical axis: relative scale.

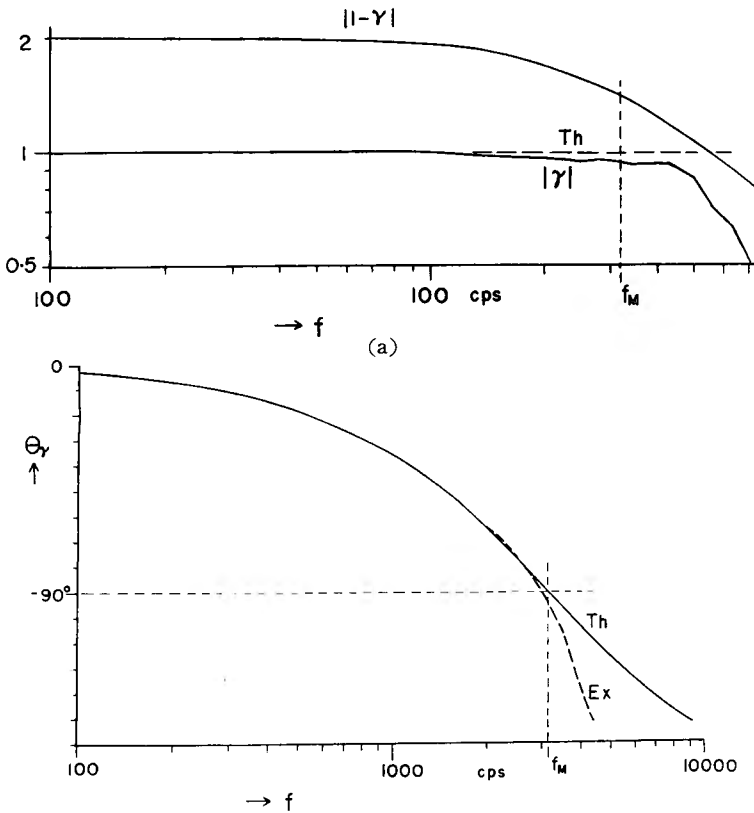


Fig. 6. (a) Values related to reflection coefficient.
 $|\gamma|$: reflection coefficient evaluated from experiment,
 T_h : theoretical reflection coefficient $|\gamma|$, $|1-\gamma|$: theoretical.
 (b) Phase angle of $-\gamma$, θ_γ .
 E_x : experimental, T_h : theoretical, f_M : f where $\omega M/(\rho CS)=1$.

one piece of paper at the same time. $\bar{\epsilon}_l$ and $\bar{\epsilon}_R$ were evaluated by eliminating the attenuation effect from $\bar{\epsilon}_i$ and $\bar{\epsilon}_r$. This elimination was done by comparing the above $\bar{\epsilon}_i$ and $\bar{\epsilon}_r$ with $\bar{\epsilon}_i$ and $\bar{\epsilon}_r$ obtained in the condition, the geophone end being free (the end part of the bar containing the geophone was cut off). By this procedure $|\bar{\gamma}| = |\bar{\epsilon}_R|/|\bar{\epsilon}_l|$ was evaluated. This is shown in Fig. 6.

Phase angles of $\bar{\epsilon}_l$ and $\bar{\epsilon}_R$ were evaluated from those of $\bar{\epsilon}_i$ and $\bar{\epsilon}_r$ by using Eq. (11) and (12). It was otherwise ascertained that propagation velocity did not depend on frequency in the range from 100 to 10000 cps, and was practically constant, i.e. 1.63~1.65 km/s. r was measured as the distance between the center of the strain gauge and the bottom of the geophone. Evaluated phase angle of $-\bar{\gamma}$ regarding experimental data is demonstrated with the theoretical curve (Fig. 6 (b)). In the theoretical evaluation Eq. (15) was applied on the assumption that the end part containing the geophone was regarded as a rigid body, 89 g in mass. The outer case of the geophone body was made of iron and was rigid enough compared with the wave bar. The mass of the geophone alone was 50 g.

The experimental values of $|\bar{\gamma}|$ coincide with the theory up to 4000 cps, those of θ_γ up to 3000 cps. Hence, at least up to 3000 cps coupling between the geophone and the bar was practically complete in the present experiment. From Eq. (19) and (17), particle velocity, \bar{V} , of the geophone body was evaluated by using the theoretical $\bar{\gamma}$.

In order to evaluate E_h we must know the usual geophone constants which make it possible to construct the lower frequency characteristics of the geophone. The constants measured otherwise (vibration table, step force method (Kitsunetzaki *et al.* [1964])) are as follows:

$$f_0 = 29.6 \text{ cps}$$

$$h = 0.41 \text{ (load resistance } R = 200 \Omega)$$

$$R_0 = 215 \Omega$$

$$G = 0.100 \text{ V/kine } \pm 5\%$$

$$A_0 = 0.482 \text{ V/kine } \pm 5\% \text{ (} R = 200 \Omega)$$

where f_0 is the natural frequency.

Using the above constant, f_0 and h , we can evaluate $A_l (= E_l)$ by Eq. (44). From Eq. (30) and the first equation of Eq. (24), we can evaluate " $E_0 E_h(t)$ ". " $E_0 E_l(t)$ " and " $E_0 E_h(t)$ " are illustrated with $E(t)$ in Fig. 4.

The value of E_0 evaluated as an integration of the above " $E_0 E_h(t)$ " should coincide with the value of E_0 evaluated from the first equation of Eq. (24). In this experiment the ratio of the former to the latter was 0.94. The error is permissible if the degree of accuracy of this experiment is considered.

We shall define \bar{A}_h as

$$\bar{A}_h = \frac{\bar{E}_h}{\bar{V}_H}$$

Hence, from Eq. (22) and (24).

$$A_0 \bar{A}_h = \frac{E_0 \bar{E}_h}{\bar{V}}$$

“ $A_0 \bar{A}_h$ ” was directly evaluated by using the above equation. When $A_0 \bar{A}_L$ was computed (Fig. 7), $A_0 = 0.094$ V/kine was tentatively applied as to fit the evaluated value of “ $E_0 \bar{E}_h(0)$ ”.

In the frequency range of $f > 300$ cps, \bar{E}_h can be regarded as \bar{E}_H with accuracy of $\pm 2\%$. With the same accuracy in this frequency range,

$$\bar{A}_h = \bar{A}_H.$$

It is expected that we can completely convert \bar{E}_h to \bar{E}_H by using Eq. (28). In the present experiment, however, this has no meaning, because longer analysis duration, t_h , is necessary in order to obtain complete $\bar{E}_h(\omega)$ which has sufficient accuracy in the lower frequency range.

If we formally convert \bar{E}_h to \bar{E}_H in the frequency near 100 cps, $|\bar{E}_h|$ decreases by about 10% from $|\bar{E}_h|$. Therefore, since $A_0 \bar{A}_H$ must match with $A_0 \bar{A}_L$, exact \bar{E}_h should be larger than the present \bar{E}_h in this frequency. Generally, in the frequency range where \bar{E}_h does not coincide with \bar{E}_H , \bar{E}_h is expected to have particular form affected by interference of \bar{E}_H and \bar{E}_L . This also affects the form of $E_h(t)$. In order to evaluate such an effect of $E_h(t)$, at least one period which corresponds to the frequency must be free from noisy phenomena.

Consequently, we assume :

$$\bar{A} = A_0 \bar{A}_L \quad f < 100 \text{ cps,}$$

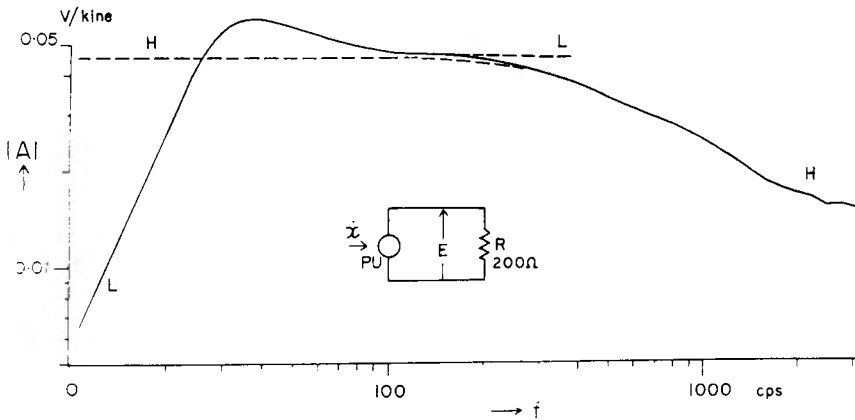


Fig. 7. Overall characteristics of the tested geophone (V1) evaluated from the present experiment (accuracy: $\pm 10\%$).

$H-H$; $A_0 \bar{A}_h$, $L-L$; $A_0 \bar{A}_L$

$$\bar{A} = A_0 \bar{A}_h \quad f > 300 \text{ cps.}$$

For $100 < f < 300$ cps, \bar{A} is drawn by naturally connecting $A_0 \bar{A}_L$ and $A_0 \bar{A}_h$. The final frequency characteristics of the tested geophone is demonstrated in Fig. 7.

3. Discussion and Conclusion

Generally, absolute exact measurement of motion of a vibration body is a troublesome problem in the higher frequency range. It is, however, still more difficult to assure coincidence of motion between the geophone to be tested and vibration table. Coupling of any bodies is not completely rigid in general. Elastic compliance which exists at contact surface of the bodies becomes effective in the higher frequency range. Hence, we cannot always assure that motion of the geophone to be tested coincides with that of the vibration table.

This fundamental difficulty has been overcome in the present method, because the reflection coefficient can be used as the indicator to ascertain the coupling condition of the geophone.

One may doubt the accuracy of the strain detector in the higher frequency range. We can easily assure the safety frequency range, where the strain gauge exactly follows the strain variation, by the following method.

For convenience in Fig. 2, we shall assume that \bar{V} is strain, \bar{A} is the characteristics of the strain detector, and hence \bar{E} is the output response of the strain detector. \bar{A} is assumed to have so-called "high cut characteristics". Its "low cut characteristics" has essentially no meaning, because the strain gauge itself has no low cut characteristics. The strain spectrum is also assumed to have "high cut characteristics". The "high cut frequency" of \bar{E} becomes lower than that of \bar{A} and the strain. If the "high cut frequency" of the strain is sufficiently higher than that of \bar{A} , the "high cut frequency" of \bar{E} coincides with that of \bar{A} . So, we can safely assure that the strain detector has constant sensitivity at least up to the "high cut frequency" of the response when isolated strain pulse having the form as \bar{V} in Fig. 2 is applied. Of course it is desirable that the time width of the input strain pulse is as short as possible. By this method we could ascertain that the strain gauge (wire resistance, paper base) has constant sensitivity at least in the frequency range of the present experiment.

In the condition of geophone set illustrated in Fig. 3, the highest frequency limit, up to which accuracy of the measurement was assured, was at least 3000 cps. When the geophone to be tested was directly adhered to the end of the wave bar, this limit was otherwise ascertained to be at least 4000 cps. The author believes that those figures do not mean essential limit of this

method. They have meaning only in the present experiment. If we improve technical details of the experiment, for example, distortion of the recording system, the frequency limit can be higher.

In the practical application of this method, selection of the wave bar material is the most important problem. We should pay attention to the following factors. At first we should adjust the acoustic impedance of the bar as to obtain relatively proper value compared with that of the geophone body to be tested. The propagation velocity, the attenuation and the length of the bar should be also considered.

When we observe the high frequency waves, it becomes the most important problem to avoid the higher order resonance of the geophone. We can assure that the present tested geophone has not the resonances of the higher order, at least considerable ones, up to 4000 cps.

Acknowledgement

The author thanks his fellow researcher, Mr. Isamu Hirano, who helped him with his computer techniques.

References

- Kitsunozaki, C. and H. Koseki, 1960; New pick-up for high frequency seismic prospecting, *Butsuritanko*, 13, 244-245.
- Kitsunozaki, C., 1960; Study on high frequency seismic prospecting (1), *ibid.*, 13, 102-107, 137-146 (in Japanese).
- Kitsunozaki, C., 1960; Study on high frequency seismic prospecting (2), *ibid.*, 13, 185-193.
- Kitsunozaki, C., 1961; Study on high frequency seismic prospecting (3), *ibid.*, 14, 125-129.
- Kitsunozaki, C., 1963; High frequency seismic prospecting, *Geophysical Papers Dedicated to Prof. K. Sassa, Geophys. Inst., Kyoto Univ.*, 179-185.
- Kitsunozaki, C. and N. Goto, 1964; On the determination of geophone characteristics by "step force method", *Butsuritanko*, 17, 166-175 (in Japanese).